

A Walsh Waveform Analyzer and Its Applications to Filtering of Pulse Signals

Yoshihiro Tanada* and Hiroya Sano*

(Received February 7, 1979)

Synopsis

A new waveform analyzer based on the Walsh transform is developed and is applied to a real-time filtering of fast pulse signals, and the linear filterings of time signals through the Walsh transform is discussed.

The analyzer converts a solitary waveform during 16 μ s into the 16 Walsh amplitude spectra in a hybrid manner: it has the sequency band from 62.5 kzps to 500 kzps. The spectra are parallely held during 16 μ s by analog integrators, while serially displayed by the CRT, and one of them is digitally read out. The spectra of the test waves are measured within the error rate of several per cent.

The analyzer is applied to the correlative detection of the photoelectric pulse signals in a gas-spectroscopic system using a pulse laser, and there composes the matched filter, which is useful for measuring the signals superposed by Gaussian noises with a high accuracy.

For the real-time filtering of fast signals, the arithmetic convolution and the frequency power spectra are approximated using the complex Walsh transform. These approximations are of practical use in 16 or 32 dimensions. Then, the matched filters for

*Department of Electronics

pulse peaking are given by the approximate convolution and by the dyadic convolution.

1. Introduction

Spectral analysis of signal waveforms is one of the basic signal processings, which contributes to character extraction and filtering of signals and any other purposes. A spectrum of a signal waveform is mathematically expressed as the inner product of the waveform and the orthogonal function. In this case it is desirable that the function has the adaptability to both electronic circuits and physical systems. Recently, the frequency spectral analysis by the sinusoidal functions is executed on the digital real-time processor¹⁾, where the fast Fourier transform (FFT) drastically reduces the number of multiplications but the frequency in the real-time execution remains in audio band because of time consumption of each multiplication.

In the pulse appliances such as the radar, the laser-radar (lidar) and the sonar, or in the general fast-signal systems, the real-time spectral analysis may be executed by the simpler orthogonal functions. The Walsh orthogonal functions take only two values ± 1 and the multiplications in the Walsh transform are replaced with additions and subtractions²⁾. Therefore, the fast Walsh transform (FWT) is more quickly computed than the FFT and utilized for the computer processings of voice and picture signals. The Walsh spectrum representation of the ordinary or arithmetic convolution, however, presents so complicated aspect³⁾, that the application of the non-modified Walsh transform to the filtering described as the arithmetic convolution offers few advantages, and that the real-time Walsh spectrum analyzer was not developed for the general signal processing until recently.

With the intent to approximate the arithmetic convolution using the modified simple and quick Walsh transform, we develop a new Walsh waveform analyzer, which transforms a near-video pulse signal during 16 μ s into 16 Walsh amplitude spectra in real time not with the FWT but with the pulse-width modulation⁴⁾. We utilize it for the correlative detection of photoelectric signals in a spectroscopic system using a pulse laser⁵⁾. And we discuss the Walsh filtering of the ordinary signals in the time-invariant system⁶⁾. Thus, the real-time spectral processing can be accelerated by the Walsh transform.

2. Walsh Functions and Walsh Transform

Walsh function, the complete orthogonal function taking +1 or -1 value, was created by J.L. Walsh in 1923. His original function can be expressed by Rademacher function $\{R(2^m\theta); R(\theta+1)=R(\theta), m=0,1,\dots, n-1\}$ as⁷⁾

$$\text{wal}(I,\theta) = \prod_{m=0}^{n-1} \{R(2^m\theta)\}^{I_{m+1} \oplus I_m} \quad (1)$$

where θ is independent variable within $[0,1)$ and the order $\{I; 0,1,\dots, 2^n-1\}$ has the binary representation $I=(I_{n-1},\dots, I_m,\dots, I_1, I_0)$; $I_m \in \{0,1\}$ and \oplus denotes addition modulo 2 or exclusive OR. Equation (1) is rewritten by even Walsh function $\text{cal}(i,\theta)$ and odd Walsh function $\text{sal}(i,\theta)$ of Pichler's definition as follows^{2,8)}:

$$\left. \begin{aligned} \text{cal}(i,\theta) &= \text{wal}(2i,\theta) = \prod_{m=1}^{n-1} \{ \text{cal}(2^m,\theta) \}^{i_m} \\ \text{sal}(i,\theta) &= \text{wal}(2i-1,\theta) = \text{cal}(i-1,\theta) \text{cal}(1,\theta) \end{aligned} \right\} \quad (2)$$

where $\text{cal}(2^m,\theta) = R(2^{m+1}\theta)R(2^m\theta)$ and $\text{sal}(2^m,\theta) = R(2^m\theta)$. In Fig.1 the first 16 Walsh functions are illustrated. The number of 1/2 zero-crossings within the interval $0 \leq \theta < 1$ is the sequency i which is defined by H.F. Harmuth⁹⁾. The sal and cal functions, comparable to sine and cosine functions, are generally defined for the sequency μ of real number. Now, let θ be the time variable t/T normalized by the time base T [second], and then the non-normalized sequency is $\varphi = \mu/T$ [zps; zero-cross per second]. In actual signal processing, however, the sal - cal functions of integer sequency or the wal functions are used.

For analog or digital Walsh processors, the logical expression of Walsh functions may be useful. By the mapping function of one-to-one correspondence $\{X; +1=X(0), -1=X(1)\}$, cal' and sal' of logical Walsh functions are expressed as follows⁸⁾:

$$\left. \begin{aligned} \text{cal}'(i,\theta) &= X^{-1} \{ \text{cal}(i,\theta) \} = \sum_{m=0}^{n-2} \oplus i_m \text{cal}'(2^m,\theta) \\ \text{sal}'(i,\theta) &= X^{-1} \{ \text{sal}(i,\theta) \} = \text{cal}'(i-1,\theta) \oplus \text{sal}'(1,\theta) \end{aligned} \right\} \quad (3)$$

where X^{-1} and $\sum \oplus$ denote inverse mapping and summation modulo 2 respectively.

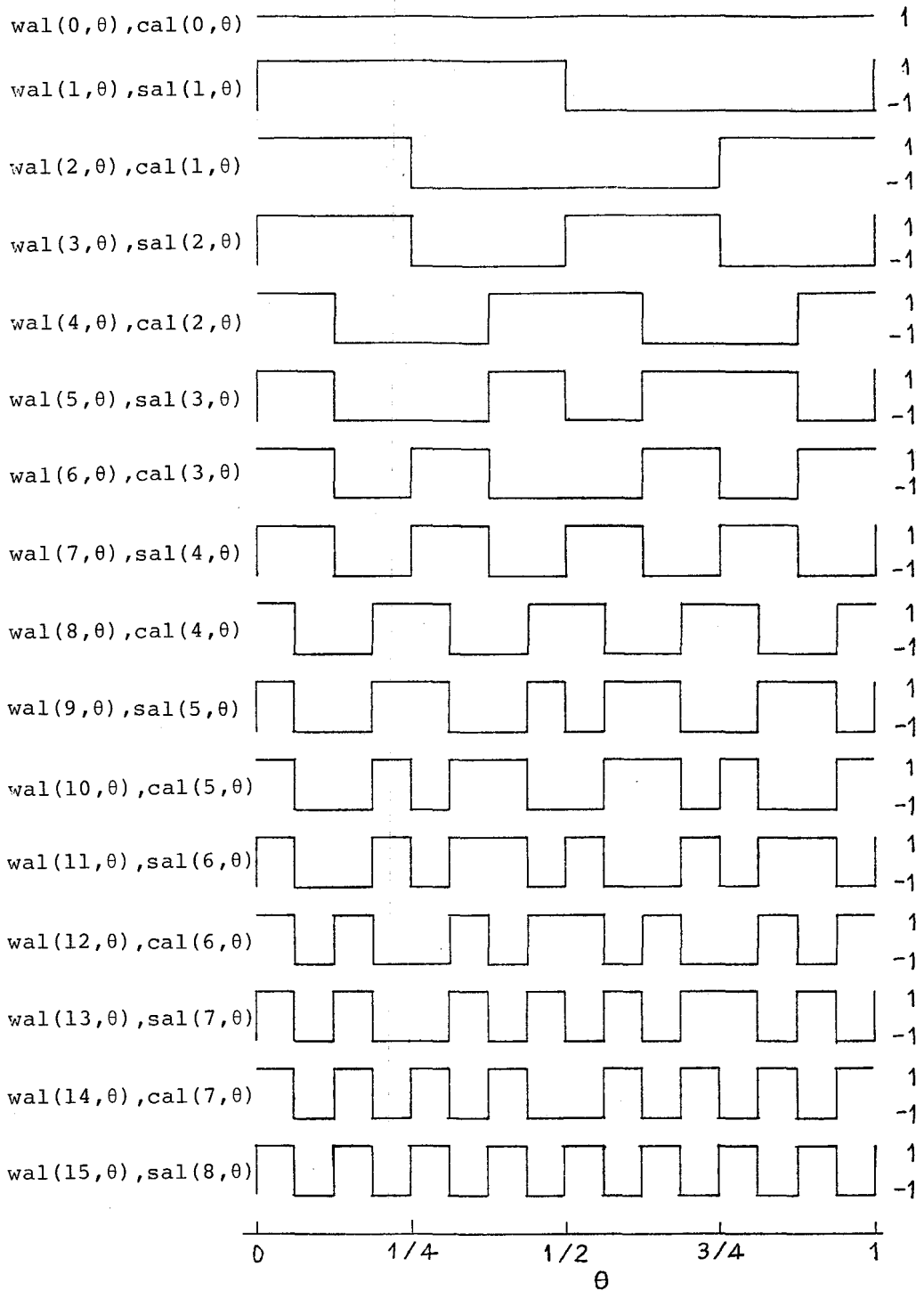


Fig.1 The first 16 Walsh functions.

The Walsh series of any waveform is ended in the first $N=2^n$ terms with computation facilities. A waveform $F(\theta)$ at the time interval $[0,1)$ is expanded in a series by the first N Walsh functions as follows:

$$\tilde{F}(\theta) = \sum_{i=0}^{N-1} a_i \text{wal}(i, \theta) \quad (4)$$

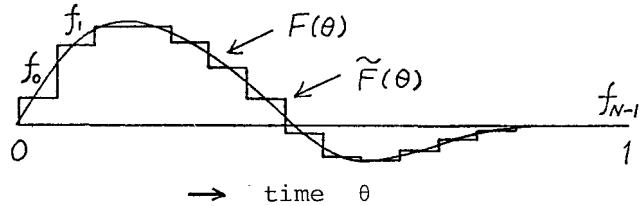
where a_i is the Walsh amplitude spectrum, represented by the Walsh transform:

$$a_i = \int_0^1 F(\psi) \text{wal}(i, \psi) d\psi \quad (5)$$

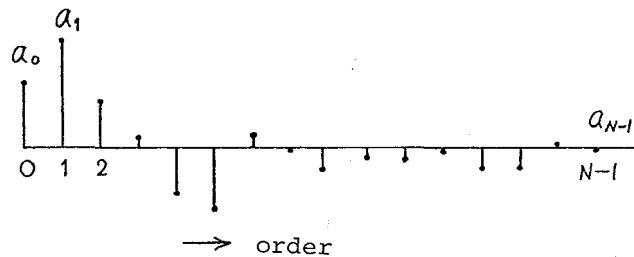
The value of the approximate waveform $\tilde{F}(\theta)$ at $k\Delta\theta \leq \theta < (k+1)\Delta\theta$ ($\Delta\theta=1/N$, $k=0,1,\dots,N-1$) is expressed by substituting Eq. (5) to Eq.(4) as the following average value:

$$\begin{aligned} f_k &= \int_0^1 F(\psi) \left\{ \sum_{i=0}^{N-1} \text{wal}(i, \theta) \text{wal}(i, \psi) \right\} d\psi \\ &= \frac{1}{\Delta\theta} \int_{k\Delta\theta}^{(k+1)\Delta\theta} F(\psi) d\psi \end{aligned} \quad (6)$$

In Fig.2 $F(\theta)$, $\tilde{F}(\theta)$ and a_i are illustrated.



(a) Walsh expansion of a waveform.



(b) Walsh amplitude spectra.

Fig.2 Walsh transform of a waveform by the first N Walsh functions.

Thus, the Walsh inverse transform and the Walsh transform take the following discrete forms of Eqs.(7) and (8) respectively

$$f_k = \sum_{i=0}^{N-1} a_i \text{wal}(i, \theta_k) \tag{7}$$

$$a_i = \Delta\theta \sum_{k=0}^{N-1} f_k \text{wal}(i, \theta_k) \tag{8}$$

where $\theta_k = \theta; k\Delta\theta \leq \theta < (k+1)\Delta\theta$. In computer execution of these transforms, the FWT algorithm is usually adopted.

3. A Walsh Waveform Analyzer for Signals of Near-Video Band

3.1 Principle

For fast and simple execution of the Walsh transform on hardware, we adopt an operation method based on the pulse-width modulation⁴⁾. The principle of the method is explained according to Fig.3. The input waveform $F(\theta)$ is averaged at every interval of $\Delta\theta$, to be $\tilde{F}(\theta)$.

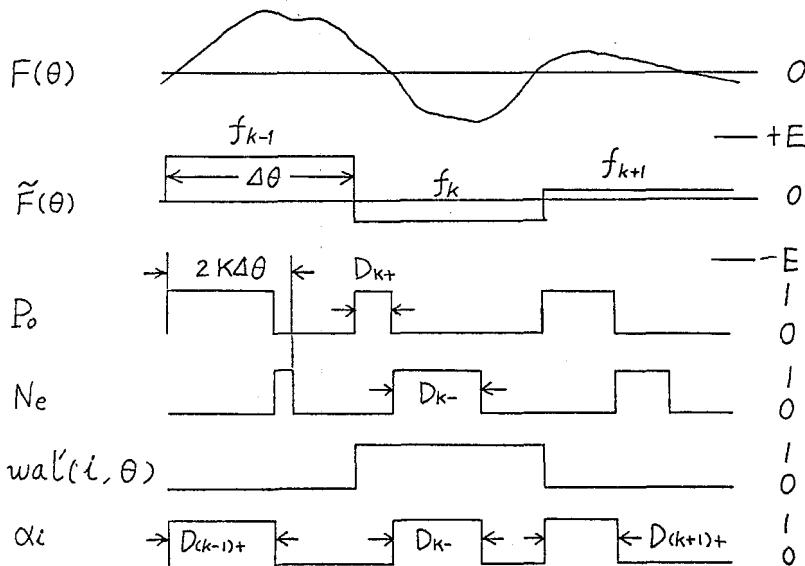


Fig.3 Operation scheme of the hybrid analyzer.

The average value $f_k (|f_k| \leq E)$ is piled up to the positive value $f_k + E$, and then it is converted to the pulse width

$$D_{k+} = K\Delta\theta (1 + f_k/E) \quad (9)$$

where $0 < K \leq 1/2$. Thus, the pulse width to the reverse value $-f_k$ is given by the complement operation

$$D_{k-} = K\Delta\theta (1 - f_k/E) = 2K\Delta\theta - D_{k+} \quad (10)$$

The pulse trains P_o and N_e consist of the pulses of D_{k+} and D_{k-} respectively. Now, the calculation of Eq.(8) is divided into two parts of multiplication and summation or integration. The multiplication is carried out as follows. The logical Walsh function $wal'(i, \theta)$ picks exclusively the pulse element out of the pulse train P_o or N_e at every interval. The logical expression of this relation is

$$\alpha_i = P_o \overline{wal'}(i, \theta) \vee N_e wal'(i, \theta) \quad (11)$$

where the pulse width at $\theta = \theta_k$ is

$$D_k = K\Delta\theta \{1 + (f_k/E) wal(i, \theta_k)\} \quad (12)$$

Integrating the durations of the truth value 1 in the hybrid signal α_i and subtracting the excess duration $NK\Delta\theta = K$ gives the quantity proportional to the Walsh amplitude spectrum a_i . The real spectrum is given by

$$a_i = \frac{E}{K} (-K + \sum_{k=0}^{N-1} D_k) = -E + \frac{E}{K} \sum_{k=0}^{N-1} D_k \quad (13)$$

In case that each pulse width D_k can be converted into the number of pulses enough to attain accuracy, accumulator (rightly named to be digital intergrator) executes the integration. Otherwise in case of high-speed analyzing, the analog serial adder (a sort of analog integrator) which takes the initial value $-E$ and the conversion coefficient $E/(KT)$ converts the hybrid signal α_i into the analog amplitude a_i . In either case, the most striking feature of this method is to execute the multiplication on digital circuit, and it can make the compact or large-scale analyzer.

Another method of the hybrid computation based on the FWT is reported by J.W.Carl and R.V.Swartwood¹⁰, but it renders the real-time processing incapable because of using many analog devices such as sample holders, adders and switches.

3.2 Prototype Analyzer

The equipment in trial, for the application to the detection of fast pulse signals, analyzes the waveform during $16\mu\text{s}$ into the 16 Walsh amplitude spectra: it has the sequency band from 62.5 kzps to 500 kzps. The specifications are listed in Table 1. The external appearance and the schematic diagram of the analyzer are shown in Figs.4

and 5 respectively. The input waveform starts to be analyzed by an external trigger pulse. The conversion of the average value f_k into the time width D_{k+} is executed alternately in two channels, on each side of which the following process is repeated eight times: the input voltage waveform is integrated during the first $1\mu\text{s}$ interval and the integrator output f_k ($|f_k| \leq E = 1\text{V}$) is held during the next 500ns interval while compared with the saw-tooth wave to be the pulse width D_{k+} ($K=1/4$) and the integrator output returns to zero in the third 500ns interval. Rearranging the two pulse trains from the channels, the multiplier yields the 16 pulse trains $\{\alpha_i; i=0,1, \dots, 15\}$ according to Eq.(11). The analog serial adder with the initial value -1V and the conversion

Table 1 Specifications of the analyzer.

Spectral number N	16
Analyzing time T	$16\mu\text{s}$
Holding time	$16\mu\text{s}$
Sequency band	62.5kzps~500kzps
Waveform amplitude f_k	-1V~+1V
Trigger pulse	Required
Single-shot waveform	Acceptable
Repetitive waveform	Acceptable
Clock frequency	16MHz

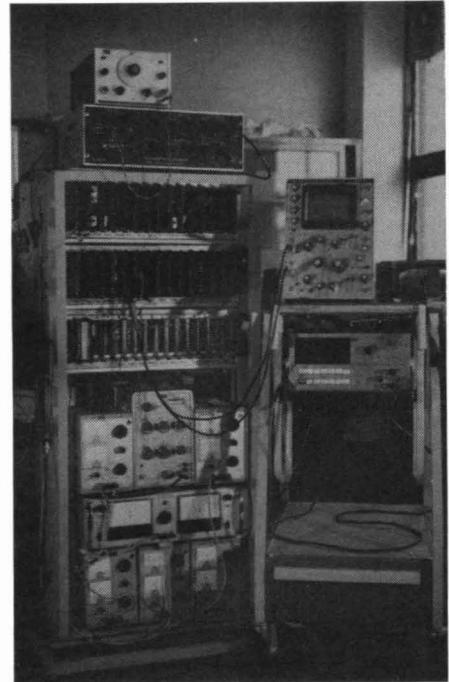


Fig.4 External appearance of the analyzer.

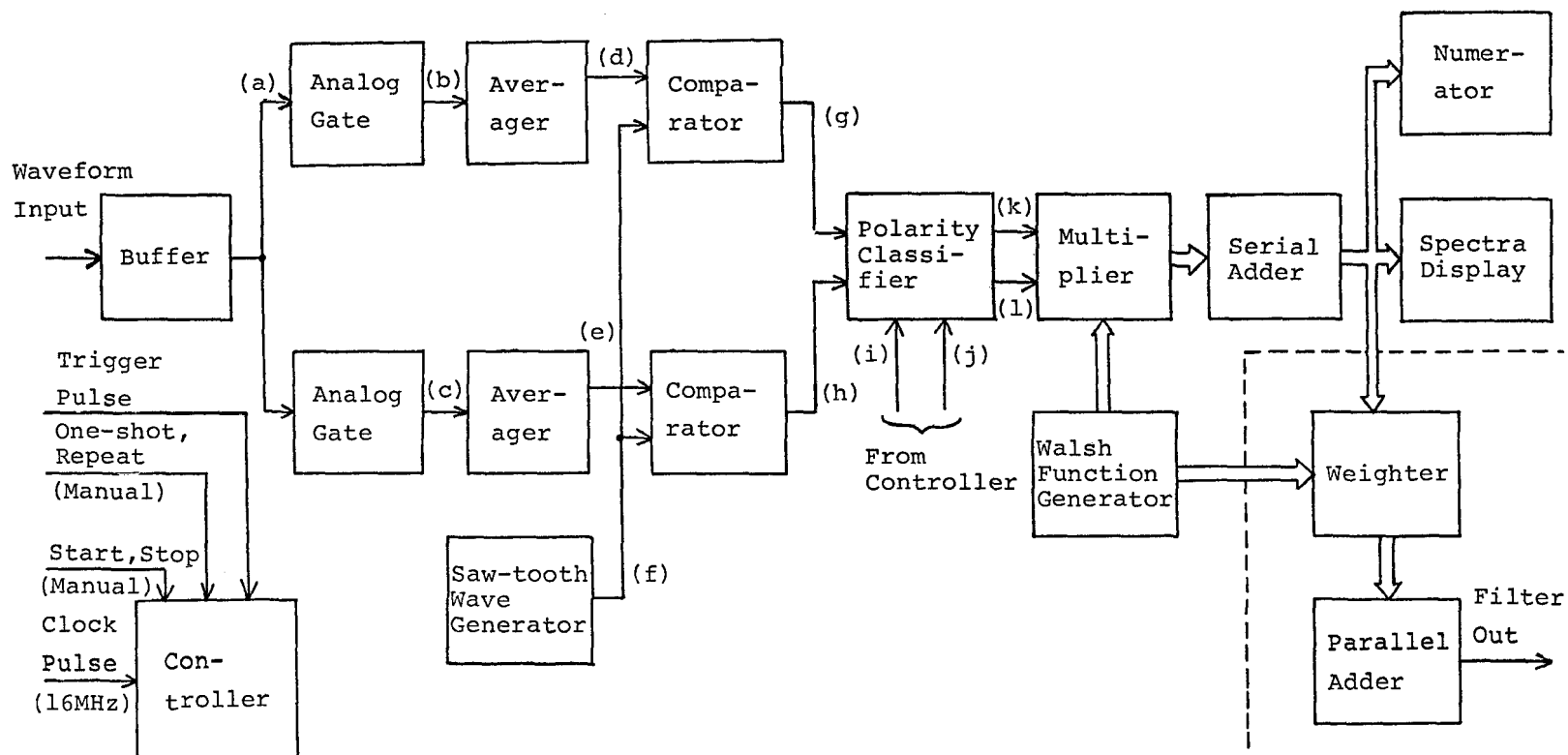


Fig.5 Schematic diagram of the analyzer.

coefficient $1/4 \text{ V}/\mu\text{s}$ converts the trains $\{\alpha_i\}$ into the 16 Walsh amplitude spectra $\{a_i; i=0,1,\dots,15\}$ at $16\mu\text{s}$ after triggering, and the spectra are held during the successive $16\mu\text{s}$ interval while they are displayed by the CRT and one of them is converted into the pulse number at the rate of $100 \text{ l}/\text{V}$ by the numerator.

3.3 Performance

The performance of the analyzer is tested by reading the output values to several solitary and continuous waveform inputs. In this case the repetition rate of the trigger pulse is 1.4 kHz asynchronous with the 16 MHz clock frequency. Fig.6 shows the oscillograms of the operating signals at the various parts of the analyzer where a synchronous 125 kHz cosine wave $\cos 4\pi t/T$ (V) is the test waveform. These oscillograms prove the good operating of the analyzer. Table

Table 2

The spectra of $\cos 4\pi t/T$.

	Analyzed values (V)	Computed values
a_0	0.04	0.000
a_1	0.01	:
a_2	0.03	:
a_3	0.03	0.000
a_4	0.75	0.637
a_5	0.03	0.000
a_6	:	:
a_7	:	:
a_8	:	:
a_9	:	:
a_{10}	0.03	:
a_{11}	0.02	0.000
a_{12}	0.29	0.264
a_{13}	0.03	0.000
a_{14}	0.03	:
a_{15}	0.02	0.000

2 shows the analyzed and the computed values of the spectra of the cosine wave.

Fig. 7 shows the oscillogram of the displayed spectra where an asynchronous 217.5 kHz , 2 V peak-to-peak sinusoidal wave is the test waveform. The maximum value of

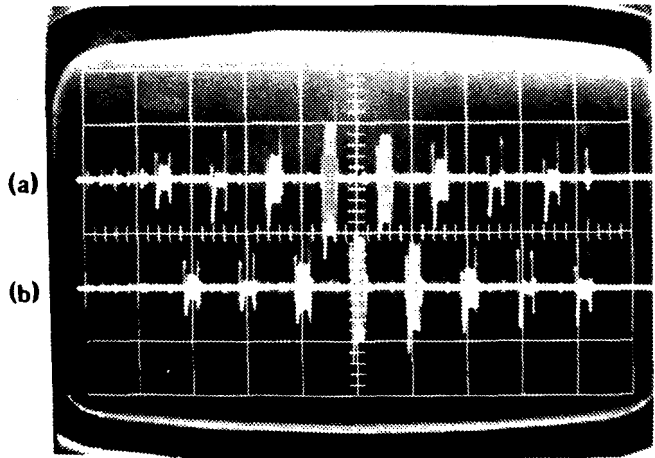


Fig.7 Oscillogram of the spectra of an asynchronous 217.5 kHz , 2 V p-p sinusoidal wave. (a) Even spectra. (b) Odd spectra.

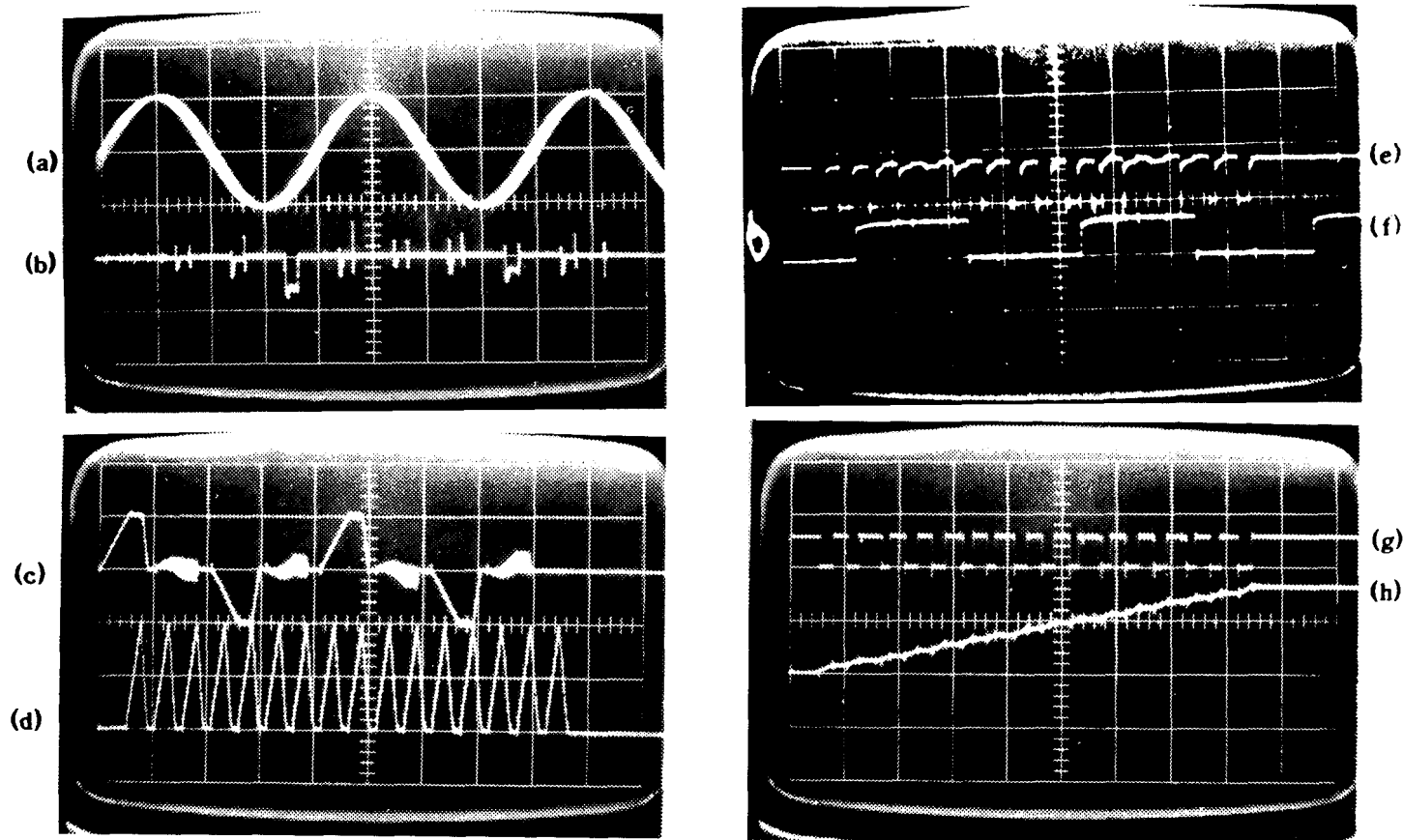


Fig.6 Oscillograms of the operating signals on the analyzer.

(a) Input waveform. (b) Even frequency amplitude spectra (inverted). (c) Averager output of the first channel (see Fig.5(d)). (d) Saw-tooth wave (see Fig.5(f)). (e) \bar{P}_0 (see Fig.5(k)). (f) $\text{wal}'(4,t/T)$. (g) $\bar{\alpha}_4$. (h) The fifth output of the serial adder. The scales of (a) to (d) and (h) : $2 \mu\text{s}/\text{div.}, 1 \text{ V}/\text{div.}$ The scales of (e) to (g) : $2 \mu\text{s}/\text{div.}, 5 \text{ V}/\text{div.}$

each fluctuating spectrum is represented by

$$\left. \begin{aligned} |a_c(i)|_{\max} &= \sqrt{a_{cc}^2(i) + a_{cs}^2(i)} ; i=0,1,\dots,7 \\ |a_s(i)|_{\max} &= \sqrt{a_{ss}^2(i) + a_{sc}^2(i)} ; i=1,2,\dots,8 \end{aligned} \right\} \quad (14)$$

where

$$\left. \begin{aligned} a_{cc}(i) &= \int_0^1 c a l(i, \theta) \cos 2\pi \nu \theta d\theta ; i=0,1,\dots,7 \\ a_{cs}(i) &= \int_0^1 c a l(i, \theta) \sin 2\pi \nu \theta d\theta ; i=0,1,\dots,7 \\ a_{sc}(i) &= \int_0^1 s a l(i, \theta) \cos 2\pi \nu \theta d\theta ; i=1,2,\dots,8 \\ a_{ss}(i) &= \int_0^1 s a l(i, \theta) \sin 2\pi \nu \theta d\theta ; i=1,2,\dots,8 \end{aligned} \right\} \quad (15)$$

$$\theta = t/T, \nu = T/T_s = 3.48 \quad (T=16\mu s, 1/T_s=217.5\text{kHz})$$

Table 3 shows the com-

puted maximum values. The above and the other results show that the spectra are measured

within the error of several per cent of the maximum amplitude 1 v and that the sequency resembles to the frequency.

This method has the characteristics that the processing is fast and the hardware compact and the aliasing not caused.

Table 3 The maximum sequency amplitude spectra of an asynchronous sinusoidal wave $\sin 2\pi \nu t/T$ ($\nu=3.48$).

i	$ a_c(i) _{\max}$	i	$ a_s(i) _{\max}$
0	0.091	1	0.097
1	0.042	2	0.040
2	0.191	3	0.203
3	0.469	4	0.441
4	0.359	5	0.382
5	0.165	6	0.155
6	0.032	7	0.034
7	0.079	8	0.074

4. Applications of the Analyzer to Filtering of Pulse Signals

4.1 Correlative Detection

In this section the analyzer is applied to the correlative detection of the photoelectric pulse signals in a gas-spectroscopic system using a pulse laser ⁵). A model of the correlative detector e.g. the box-car integrator or the lock-in amplifier mostly used in such a system is shown in Fig.8. Let the time functions $f(t)$, $r(t)$ and $h(t)$ be an input signal, an input noise and the weighting function respective-

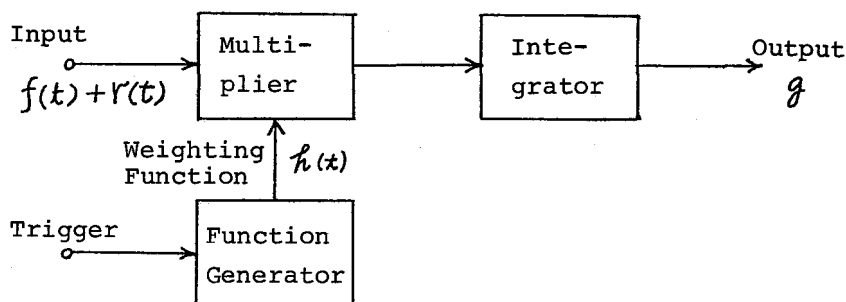


Fig. 8 A model of the correlative detector.

ly, the output in response to the single-shot input is given by the correlation integral

$$g = \frac{1}{T} \int_0^T \{f(t) + r(t)\} h(t) dt \quad (16)$$

where T is the time base as before. The functions $f(t)$, $r(t)$ and $h(t)$ are approximately expressed by the Walsh series as

$$\left. \begin{aligned} f(t) &\approx \sum_{i=0}^{15} a_i \text{wal} \left(i, \frac{t}{T} \right), & r(t) &\approx \sum_{i=0}^{15} d_i \text{wal} \left(i, \frac{t}{T} \right) \\ h(t) &\approx \sum_{i=0}^{15} c_i \text{wal} \left(i, \frac{t}{T} \right) \end{aligned} \right\} \quad (17)$$

where

$$\left. \begin{aligned} a_i &= \frac{1}{T} \int_0^T f(t) \text{wal} \left(i, \frac{t}{T} \right) dt, & d_i &= \frac{1}{T} \int_0^T r(t) \text{wal} \left(i, \frac{t}{T} \right) dt \\ c_i &= \frac{1}{T} \int_0^T h(t) \text{wal} \left(i, \frac{t}{T} \right) dt \end{aligned} \right\} \quad (18)$$

Using Eq. (17), Eq. (16) is approximately expressed as

$$g = \sum_{i=0}^{15} a_i c_i + \sum_{i=0}^{15} d_i c_i \quad (19)$$

Thus, the detector model of Fig. 8 can be modified to the Walsh processing model shown in Fig. 9.

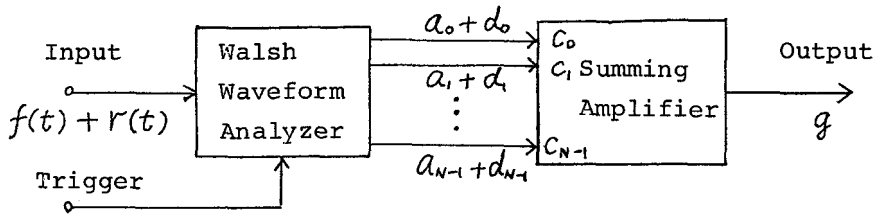


Fig.9 The correlative detector using the Walsh waveform analyzer.

The weighting function of the box-car integrator or the lock-in amplifier is, for example, $h(t) = 16[u(t-k\Delta t) - u\{t-(k+1)\Delta t\}]$ ($k=0,1,\dots,15$) or $h(t) = \text{wal}(1, t/T)$ respectively, and they are rather fixed. Generally, an appropriate weighting function can bring the optimum detection, where it is simpler for the hardware to weight the amplitude spectra $\{c_i\}$ than to generate the time function $h(t)$.

Thus, the optimum detector for the photoelectric pulse signals in the spectroscopic system is constructed with the Walsh waveform analyzer in the following manner. In this case, the signal has the known waveform, and the noise the white-normal distribution, so the signal-to-noise ratio of the detector output is related to the Schwarz's inequality

$$\left(\sum_{i=0}^{15} a_i c_i \right)^2 / \sum_{i=0}^{15} \bar{d}_i^2 c_i^2 \leq \sum_{i=0}^{15} a_i^2 / \bar{d}_i^2 \quad (20)$$

where \bar{d}_i^2 describes the ensemble mean of the noise power spectrum d_i^2 and takes the same value for every order i ($0, 1, \dots, 15$). The signal-to-noise ratio has the maximum when

$$c_i = K w a_i \quad ; \quad K w = \text{constant} \quad (21)$$

that is

$$h(t) = K w f(t) \quad . \quad (22)$$

The optimum detector takes the weighting spectrum of Eq.(21), and this detector is one of matched filters.

The practical system for detecting the photoelectric pulse signals consists of a pre-amplifier, the matched filter, an A-D converter, an accumulator and a personal computer, and can measure the magnitude of the pulse signals on the resonance absorption in the rarefied NO_2 gas and the Raman scattering from the atmospheric N_2 gas, with a high accuracy especially owing to the matched filter.

4.2 Convolution Filtering

In this section the convolution filterings of time signals using the Walsh transform are discussed ⁶⁾. The waveforms $F(\theta)$, $H(\theta)$ and $G(\theta)$ isolated at the time interval $[0, 1)$ are expanded in the Walsh series to be $\tilde{F}(\theta)$, $\tilde{H}(\theta)$ and $\tilde{G}(\theta)$ of which spectra are a_i , c_i and b_i , respectively. Now, these waveforms are assumed to repeat with the period 1. If $\tilde{F}(\theta)$ is an input to the dyadic-invariant system with the impulse response $\tilde{H}(\theta)$, then the output $\tilde{G}(\theta)$ is represented by a finite dyadic convolution:

$$\tilde{G}(\theta) = \Delta\theta \sum_{k=0}^{N-1} \tilde{F}(\theta_k) \tilde{H}(\theta \oplus \theta_k) \quad (23)$$

where $\Delta\theta = 1/N$, $N=2^n$, $\theta_k = \{\theta; k\Delta\theta \leq \theta < (k+1)\Delta\theta, k=0,1,\dots,15\}$, $\theta = \{\theta; \ell\Delta\theta \leq \theta < (\ell+1)\Delta\theta, \ell=0,1,\dots,15\}$ and the dyadic shift $\theta \oplus \theta_k = \Delta\theta(\ell \oplus k)$. The Walsh amplitude spectrum of $\tilde{G}(\theta)$ is simply represented by

$$b_i = a_i c_i \quad (24)$$

Likewise, the output $\tilde{G}(\theta)$ from the time-invariant system is represented by a finite arithmetic convolution :

$$\tilde{G}(\theta) = \Delta\theta \sum_{k=0}^{N-1} \tilde{F}(\theta_k) \tilde{H}(\theta - \theta_k) \quad (25)$$

The spectrum of this output $\tilde{G}(\theta)$ presents a complicated form as follows :

$$b_i = \sum_{p=0}^{N-1} \sum_{q=0}^{N-1} a_p c_q \gamma_{ipq} \quad (26)$$

where γ_{ipq} is the expansion coefficient of an arithmetically-shifted Walsh function ³⁾;

$$\text{wal}(q, \theta - \theta_k) = \sum_{i=0}^{N-1} \sum_{p=0}^{N-1} \gamma_{ipq} \text{wal}(i, \theta) \text{wal}(p, \theta_k) \quad (27)$$

In this case the calculation of the spectra $\{b_i\}$ needs $(N^2+2)/3$ multiplications and additions.

For a compact approximation to the arithmetic convolution, we define the complex Walsh functions as

$$\left. \begin{aligned} W(0, \theta) &= 1, \quad W(N/2, \theta) = \text{sal}(N/2, \theta) \\ W(i, \theta) &= \{\text{cal}(i, \theta) + j\text{sal}(i, \theta)\} / \sqrt{2}; \\ j^2 &= -1, \quad |i| = 1, 2, \dots, N/2-1 \end{aligned} \right\} \quad (28)$$

and a pair of the complex Walsh transforms as

$$\left. \begin{aligned} \tilde{F}(\theta) &= \sum_{i=-(N/2-1)}^{N/2} A(i)W(i,\theta) \\ A(i) &= \Delta\theta \sum_{k=0}^{N-1} \tilde{F}(\theta_k)W^*(i,\theta_k) \end{aligned} \right\} \quad (29)$$

where the asterisk denotes the conjugate complex. $\tilde{G}(\theta)$ and $\tilde{H}(\theta)$ also take $B(i)$ and $C(i)$ respectively. Thus, the output from the time-invariant system is approximated by

$$\tilde{G}(\theta) = \sum_{i=-(N/2-1)}^{N/2} A(i)C(i)W(i,0)W(i,\theta) \quad (30)$$

where $A(i) \cdot C(i) \cdot W(i,0) = B(i)$ is the sequency amplitude spectrum and $|A(i)|^2 \cdot |C(i)|^2 = |B(i)|^2$, the sequency power spectrum. The approximation error of the arithmetic convolution is given by the square of the Hilbert-Schmidt's norm of the difference between the ideal output $H(\theta-\theta_k)$ and the approximate output

$$\hat{H}(\theta-\theta_k) = \sum_{i=-(N/2-1)}^{N/2} C(i)W^*(i,\theta_k)W(i,0)W(i,\theta) \quad (31)$$

when the time-invariant system receives the impulse input delayed by θ_k . On the other hand, the approximation error of the frequency power spectrum is given by the square mean of the difference between the absolute value $|C'(i)|$ of the frequency amplitude spectrum and the absolute value $|C(i)|$ of the sequency amplitude spectrum.

From calculating their errors for some waveform examples, it is concluded that the approximations to the arithmetic convolution and the frequency power spectrum are of practical use in the dimension $N=16$ or 32 where the latter approximation is better than the former.

The intermediate use of Eq.(31) gives the following relation between the autocorrelation function and the sequency power spectrum:

$$\left. \begin{aligned} \psi_{HH}(\theta) &= 2 \sum_{i=0}^{N/2-1} |C(i)|^2 \text{cal}(i,\theta) \\ |C(i)|^2 &= \frac{1}{2} \int_0^1 \psi_{HH}(\theta) \text{cal}(i,\theta) d\theta \end{aligned} \right\} \quad (32)$$

which is compared with the Wiener-Khintchine's theorem.

The dyadic-invariant system and the approximate system to the

time-invariant system can be utilized as the matched filters in the pulse appliances such as the radar, the lidar and the sonar. Assuming that a white Gaussian noise superposes on a pulse signal, the matched filter which gives the maximum signal-to-noise ratio to the output pulse at $\theta = \psi$ takes its spectrum as

$$C(i) = K_1 A^*(i) W^*(i, 0) W^*(i, \psi) \quad (33)$$

based on the approximate system or as

$$c_i = K_2 a_i \text{wal}(i, \psi) \quad (34)$$

based on the dyadic-invariant system where K_1 and K_2 are constant.

Fig.10 shows the general filter using the Walsh transform i.e. the sequency filter. The fast Walsh waveform analyzer and synthesizer, or the fast A-D and D-A converters and the fast microcomputer may quickly execute the above-mentioned filterings.

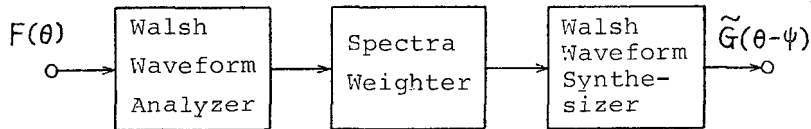


Fig.10 The sequency filter.

5. Conclusion

The high-speed and simple Walsh waveform analyzer has been newly developed and has been applied to the detection of the photoelectric pulse signals in the laser-spectroscopic system. And the linear filtering of time signals using the Walsh transform has been studied. The real-time spectral analysis can be more quickly executed by the Walsh transform than by the Fourier transform and the Walsh processor can be applied to the pulse appliances such as the radar, the lidar and sonar or to the general fast-signal systems.

Acknowledgement

We would like to thank Prof. Jun-ichi Ikenoue of Kyoto University for his continuing guidance and helpful advice. We wish to thank our seminar staffs for their experimental assistances.

References

- (1) M.Tokoro, H.Mori, N.Kaneko, M.Shimada, S.Uchida and H.Aiso: "Fast Fourier transform by hardware", Trans. IECE of Japan, 58-D (1975), 9, 578.
- (2) H.F.Harmuth: "Transmission of information by orthogonal functions", Springer Verlag (1972), 22.
- (3) Y.Tanada and H.Sano: "Walsh spectra of time-shifted waves", Trans. IECE of Japan, 57-D (1974), 8, 503.
- (4) Y.Tanada and H.Sano: "A hybrid Walsh waveform analyzer", Trans. IECE of Japan, J59-D (1976), 2, 101.
- (5) H.Sano, Y.Tanada, R.Koga and T.Ono: "Method of narrow pulsed laser light detection applied to the monitoring of air pollutions", J.Illum. Eng. Inst. of Japan, 61 (1977), 3, 159.
- (6) Y.Tanada and H.Sano: "Linear filtering of time signals using the Walsh transform", Trans. IECE of Japan, J61-A (1978), 6, 596.
- (7) R.B.Lackey and D.Meltzer: "A simplified definition of Walsh functions", IEEE Trans. Comput., C-20 (1971), 2, 211.
- (8) H.Sano and Y.Tanada: "Logical Walsh functions", Trans. IECE of Japan, 56-D (1973), 9, 531.
- (9) H.F.Harmuth: "A generalized concept of frequency and some applications", IEEE Trans. Inf. Theory, IT-14(1968), 375.
- (10) J.W.Carl and R.V.Swartwood: "A hybrid Walsh transform computer", IEEE Trans. Comput., C-22 (1973), 7, 669.